Biophysical Chemistry 139 (2009) 116–122

Contents lists available at ScienceDirect

Biophysical Chemistry

journal homepage: http://www.elsevier.com/locate/biophyschem

A systematic study on hydrogen bond interactions in sulfabenzamide: DFT calculations of the N-14, O-17, and H-2 NQR parameters

Ahmad G. Nozad [a,*], Hamidreza Najafi [a], Sakineh Meftah [b], Mustafa Aghazadeh [a,b,*]

[a] Material Research School, NSTRI, P.O. Box:14395-836, Tehran, Iran
[b] Applied Chemistry Research Group, ACECR-Tehran branch, P.O. Box: 13145-186, Tehran, Iran

ARTICLE INFO

Article history:
Received 2 September 2008
Received in revised form 26 October 2008
Accepted 27 October 2008
Available online 10 November 2008

Keywords:
Sulfabenzamide
Hydrogen bond interaction
DFT
Electric field gradient tensor
Asymmetry parameter

ABSTRACT

A systematic computational study was carried out to characterize the hydrogen bond, HB, interactions of sulfabenzamide crystal structure by DFT calculations of electric field gradient, EFG, tensors at the sites of ^{14}N, ^{17}O, and ^{2}H nuclei. The computations were performed with the B3LYP and B3PW91 DFT methods and 6-311+G* and 6-311++G** standard basis sets using the Gaussian 98 package. To perform the calculations, a hydrogen-bonded heptameric cluster of sulfabenzamide was created by X-ray coordinates where the hydrogen atom positions were optimized and the EFG tensors were calculated for the target molecule. Additional optimization and EFG calculations were also performed for crystalline monomer and an isolated gas-phase sulfabenzamide. The calculated EFG tensors were converted to the experimentally measurable nuclear quadrupole resonance, NQR, parameters: quadrupole coupling constant, C_Q, and asymmetry parameter, η_Q. The results reveal that the geometrical and NQR parameters of the optimized isolated gas-phase and crystalline phase are different. In addition, the difference between the calculated NQR parameters of the monomer and the target molecule shows how much H-bonding interactions affect the EFG tensors of each nucleus. The evaluated NQR parameters reveal that due to the contribution of the target molecule to N–H…O and C–H…O hydrogen bond interactions, the EFG tensors at the sites of N(1), O(3) and H(1) undergo significant changes from monomer to the target molecule in cluster. These features reveal the major role of N–H…O type intermolecular HBs in cluster model of sulfabenzamide which the presence of these interactions can lead to polymorphism directly related to the drug activity and related properties.

1. Introduction

Hydrogen bonds, HBs, play an essential role in natural phenomena, especially in the biological and biochemical systems [1–3]. Polymorphism, tableting behavior, and drug activity of sulfonamides, for example, is due to the formation of a network of intra- and intermolecular HBs [3–6]. In many cases, the type of these HBs is N–H…O and N–H…N which is mainly electrostatic with some charge transfer, induce, and polarization in nature. Thus, due to the importance, the nature of HB interactions has been extensively investigated by either experimental or theoretical studies up to now [7–11]. However, nuclear quadrupole resonance, NQR, spectroscopy is among the most important and versatile techniques for this purpose. Since the most characteristic nature of HB interactions is electrostatic, electric field gradient (EFG) tensors originated at the sites of quadrupole nuclei are proper elements to characterize the properties of different types of HB interactions in the solid phase [12–15]. It is noted that the quadrupole nuclei are those with spin angular momentum greater than one-half, $I>1/2$, which the interaction energy of the nuclear electric quadrupole moment, eQ, and the EFG tensors is measured by NQR as quadrupole coupling constant, C_Q. Asymmetry parameter, η_Q, indicating the EFG tensors deviation from cylindrical symmetry at the site of quadrupole nucleus is also measured by NQR.

It is an interesting subject to investigate the effects of long-range interactions such as hydrogen bonding, H-bonding, in sulfonamides and its derivatives because of their key role in the polymorphism, tableting behavior, and drug activity. Moreover, understanding the nature of these interactions can be crucial in describing the function of these systems in biological media at the molecular level. Sulfonamides are included in a main class of drugs which exhibit interesting solid-state properties due to their capability of contributing to different H-bonding interactions [5,16,17]. The importance of sulfonamides is well-established in pharmaceutical chemistry and drug design. Aromatic derivatives of sulfonamide exhibit a wide range of bioactivities such as anti-angiogenic, anti-tumor, anti-analgestic, anti-tubercular, anti-glaucoma, anti-HIV, cytotoxic, anti-microbial, and anti-malarial agents [18–30]. Sulfabenzamide is one of the most used derivatives also having anti-bacterial properties. Numerous experimental techniques including X-ray, neutron diffraction,

* Corresponding authors. Tel.: +98 21 8206 3118; fax: +98 21 8206 3112.
E-mail addresses: anozad@aeoi.org.ir (A.G. Nozad), m_aghazadeh@modares.ac.ir (M. Aghazadeh).

0301-4622/$ – see front matter © 2008 Elsevier B.V. All rights reserved.
doi:10.1016/j.bpc.2008.10.010

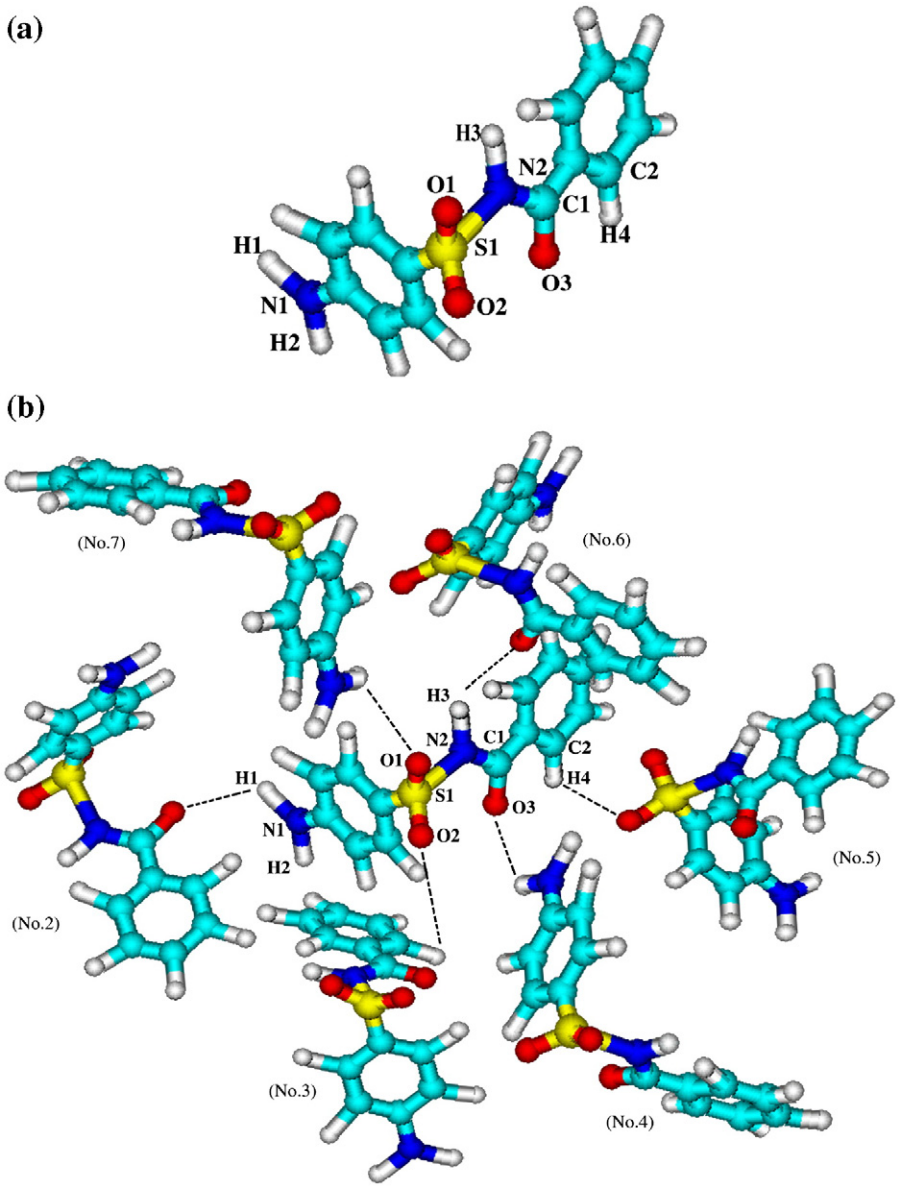

Fig. 1. (a) Monomer and (b) illustration of intermolecular hydrogen bonds in the crystalline sulfabenzamide. Dashed lines show HB interactions of the target molecule in cluster.

infrared, Raman, and NMR spectroscopies have been applied to study the nature of H-bonding interactions in sulfonamides and its derivatives in the solid phase [31–37]. The study of the contribution of 39 crystal structures of sulfonamide to HB interactions by Adsmond and Grant [4], using graph set notation, revealed that the amido protons show a greater preference of HB interactions with amidine nitrogens and cocrystal guests whereas the amino protons show a greater preference of hydrogen bonding with sulfonyl oxygens. From their work, it can be concluded that the polymorphic change resulted in a change in the hydrogen-bond pattern of the amido proton, implicated as a major player in the polymorphic transformation. The solid-state properties of sulfonamides have been studied by Yang et al. who postulated that the presence of various HBs in the sulfonamide drugs can lead to polymorphism that is related directly to the drug activity [5]. Kosutić and co-workers [38] having been studied the supramolecular three isomeric structures of sulfonamide indicated that these structures differ in their hydrogen-bonding arrangements, but in all of them the conformation of sulfonamide moiety is conserved by an intra-molecular N–H…O hydrogen bond and a C–H…O interaction. Also, our pervious density functional theory, DFT, study showed the major role of HB interactions on structural properties and NQR parameters of sulfamerazine [39].

Blinc et al. [40] who measured experimentally the ^{14}N NQR parameters of sulfonamides demonstrated the importance of regarding the N–H…N type hydrogen bond interactions in assigning the ^{14}N quadrupole coupling constant and asymmetry parameter in sulfonamides.

The present work includes a systematic computational study of HBs interactions of sulfabenzamide crystal structure via DFT calculations of the ^{14}N, ^{17}O, and ^{2}H EFG tensors. The available crystal coordinates of sulfabenzamide were obtained from previous X-ray diffraction study [41]. Considering the presence of hydrogen bonds (N–H…O and C–H…O) in the calculations, the most probable interacting molecules with the central molecule in the crystalline structure of sulfabenzamide were considered via a heptameric cluster; see Fig. 1b and Table 1 for details. To have a basis for comparison of H-bonding effects on the EFG tensors, the calculations were also performed on the monomer sulfabenzamide. All calculations were carried out at B3LYP and B3PW91 levels using 6-311+G* and 6-311++G** basis sets. The calculated EFG tensors at the sites of ^{14}N, ^{17}O,

Table 1
The structural properties of sulfabenzamide

Geometrical parameters	Fully optimized isolated gas-phase	Crystalline monomer[a]	Crystalline monomer[b]	Target molecule[c]	Intermolecular geometrical parameters[d]	Cluster model[e]
r_{N1-H1}	1.02 Å	0.99 Å	1.04 Å	1.17 Å	$r_{N1...O(3-2)}$	2.69 Å
r_{N1-H2}	1.01 Å	0.95 Å	1.02 Å	1.02 Å	$r_{N2...O(3-6)}$	2.85 Å
r_{N2-H3}	1.03 Å	1.09 Å	1.01 Å	1.11 Å	$r_{O1...N(1-7)}$	2.81 Å
r_{N2-C1}	1.42 Å	1.51 Å	1.51 Å	1.51 Å	$r_{O2...C(2-3)}$	2.98 Å
r_{N2-S1}	1.65 Å	1.59 Å	1.59 Å	1.59 Å	$r_{O3...N(1-4)}$	2.74 Å
r_{C1-O3}	1.33 Å	1.42 Å	1.42 Å	1.42 Å	$r_{C2...O(2-5)}$	3.01 Å
r_{C2-H4}	1.01 Å	1.01 Å	1.03 Å	1.10 Å	$r_{H1...O(2-2)}$	1.62 Å
r_{S1-O1}	1.57 Å	1.61 Å	1.61 Å	1.61 Å	$r_{H3...O(2-6)}$	1.85 Å
r_{S1-O2}	1.56 Å	1.62 Å	1.62 Å	1.62 Å	$r_{H4...O(2-5)}$	2.01 Å
$\angle_{H1-N1-H2}$	108.2°	110.1°	111.1°	114.8°	$r_{O1...H(1-7)}$	1.78 Å
$\angle_{O1-S1-O2}$	118.3°	119.1°	119.1°	119.1°	$r_{O2...H(4-3)}$	1.95 Å
$\angle_{H3-N2-S1}$	114.3°	112.1°	113.1°	113.9°	$r_{O3...H(1-4)}$	1.99 Å
$\angle_{H3-N2-C1}$	109.8°	108.4°	108.4°	108.2°	$\angle_{N1-H1...O(2-2)}$	156.6°
$\angle_{N2-C1-O3}$	123.4°	123.8°	123.8°	123.8°	$\angle_{N2-H3...O(3-6)}$	131.5°
					$\angle_{C2-H4...O(2-5)}$	169.8°
					$\angle_{O1...H1-N(1-7)}$	144.7°
					$\angle_{O2...H4-C(2-3)}$	103.5°

[a] Crystalline monomer is obtained by X-ray coordinates [41] before hydrogen optimization.
[b] Crystalline monomer is obtained by X-ray coordinates [41] after a geometry optimization of just hydrogen atoms at the B3LYP/6-311++G** level.
[c] The target molecule in cluster where just hydrogen positions were optimized at B3LYP/6-311++G** level.
[d] The first number in parentheses denotes the atom number and the second one denotes the molecule number; see Fig. 1.
[e] The cluster was created by transformation of X-ray coordinates, however, just hydrogen positions of cluster were optimized at the level of B3LYP/6-311++G**.

and ^{2}H nuclei were converted to the experimentally measurable NQR parameters, C_Q and η_Q, which are summarized in Tables 2–4.

2. Computational details

The DFT calculations for sulfabenzamide ($C_{13}H_{12}N_2O_3S$) were carried out by employing the GAUSSIAN 98 suite of programs [42]. This was done for calculating the EFG tensors in the principal axes system, PAS, for oxygen, nitrogen and hydrogen nuclei. Pervious works of Köster et al. [43–45] have also showed that DFT calculations are capable to reliably predict ^{14}N and ^{17}O NQR frequencies and their nuclear quadrupole coupling constants. On the other hand, among various modern functionals of DFT, B3LYP hybrid exchange-correlation functional has been proven to be the most proper and popular to

Table 2
Calculated ^{14}N quadrupole coupling tensors (MHz) and asymmetry parameters for sulfabenzamide

Model	Nucleus	Method	Basis set	χ_{xx}	χ_{yy}	C_Q	η_Q
Isolated gas-phase[a]	N(1)	B3PW91	6-311+G*	−2.10	−2.72	**4.82**	0.13
			6-311++G**	−2.09	−2.70	4.79	0.13
		B3LYP	6-311+G*	−2.07	−2.70	4.77	0.15
			6-311++G**	−2.06	−2.79	4.85	0.15
	N(2)	B3PW91	6-311+G*	−2.25	−2.45	4.70	0.04
			6-311++G**	−2.23	−2.46	4.69	0.05
		B3LYP	6-311+G*	−2.19	−2.41	4.59	0.05
			6-311++G**	−2.19	−2.42	4.59	0.05
Monomer[b]	N(1)	B3PW91	6-311+G*	−1.99	−2.65	4.64	0.17
			6-311++G**	−1.99	−2.65	4.54	0.17
		B3LYP	6-311+G*	−1.98	−2.63	4.57	0.17
			6-311++G**	−1.98	−2.64	4.60	0.17
	N(2)	B3PW91	6-311+G*	−1.89	−2.38	4.27	0.12
			6-311++G**	−1.88	−2.33	4.21	0.11
		B3LYP	6-311+G*	−1.86	−2.34	4.20	0.11
			6-311++G**	−1.86	−2.32	4.20	0.11
Cluster[c]	N(1)	B3PW91	6-311+G*	−1.07	−2.59	3.65	0.42
			6-311++G**	−1.07	−2.59	3.65	0.42
		B3LYP	6-311+G*	−1.05	−2.56	3.61	0.42
			6-311++G**	−1.02	−2.56	3.58	0.43
	N(2)	B3PW91	6-311+G*	−1.17	−2.35	3.52	0.34
			6-311++G**	−1.15	−2.32	3.47	0.36
		B3LYP	6-311+G*	−1.13	−2.35	3.48	0.35
			6-311++G**	−1.11	−2.34	3.45	0.36

[a] A fully optimized isolated gas-phase sulfabenzamide at the level of B3LYP/6-311++G**.
[b] Crystalline monomer obtained by X-ray coordinates and also optimized hydrogen positions.
[c] The target molecule in cluster.

Table 3
Calculated ^{17}O quadrupole coupling tensors (MHz) and asymmetry parameters for sulfabenzamide

Model	Nucleus	Method	Basis set	χ_{xx}	χ_{yy}	C_Q	η_Q
Isolated gas-phase[a]	O(1)	B3PW91	6-311+G*	−4.15	−6.08	10.23	0.20
			6-311++G**	−4.13	−6.07	10.20	0.19
		B3LYP	6-311+G*	−4.14	−6.04	10.18	0.19
			6-311++G**	−4.13	−6.02	10.15	0.19
	O(2)	B3PW91	6-311+G*	−3.72	−4.69	8.41	0.09
			6-311++G**	−3.72	4.69–	8.41	0.09
		B3LYP	6-311+G*	−3.69	−4.67	8.36	0.09
			6-311++G**	−3.70	−4.67	8.37	0.09
	O(3)	B3PW91	6-311+G*	−4.51	−5.11	9.62	0.06
			6-311++G**	−4.51	−5.10	9.61	0.06
		B3LYP	6-311+G*	−4.48	−5.08	9.56	0.06
			6-311++G**	−4.46	−5.07	9.53	0.06
Monomer[b]	O(1)	B3PW91	6-311+G*	−3.37	−6.68	10.05	0.33
			6-311++G**	−3.38	−6.67	10.05	0.33
		B3LYP	6-311+G*	−3.35	−6.74	10.09	0.34
			6-311++G**	−3.38	−6.70	10.08	0.34
	O(2)	B3PW91	6-311+G*	−3.71	−4.60	8.31	0.10
			6-311++G**	−3.66	−4.55	8.21	0.10
		B3LYP	6-311+G*	−3.70	−4.61	8.31	0.10
			6-311++G**	−3.69	−4.59	8.28	0.10
	O(3)	B3PW91	6-311+G*	−4.05	−5.30	9.35	0.14
			6-311++G**	−3.98	−5.36	9.34	0.15
		B3LYP	6-311+G*	−3.97	−5.36	9.33	0.15
			6-311++G**	−3.95	−5.38	9.33	0.15
Cluster[c]	O(1)	B3PW91	6-311+G*	−2.69	−7.06	9.75	0.45
			6-311++G**	−2.65	−7.07	9.72	0.46
		B3LYP	6-311+G*	−2.64	−7.09	9.71	0.46
			6-311++G**	−2.62	−7.10	9.62	0.47
	O(2)	B3PW91	6-311+G*	−3.25	−4.74	7.99	0.19
			6-311++G**	−3.33	−4.76	8.09	0.18
		B3LYP	6-311+G*	−3.35	−4.79	8.14	0.18
			6-311++G**	−3.33	−4.75	8.08	0.18
	O(3)	B3PW91	6-311+G*	−2.08	−6.57	8.65	0.52
			6-311++G**	−2.05	−6.58	8.63	0.52
		B3LYP	6-311+G*	−2.03	−6.59	8.62	0.53
			6-311++G**	−2.02	−6.57	8.59	0.53

[a] A fully optimized isolated gas-phase sulfabenzamide at the level of B3LYP/6-311++G**.
[b] Crystalline monomer obtained by X-ray coordinates and also optimized hydrogen positions.
[c] The target molecule in cluster.

Table 4
Calculated ^{2}H quadrupole coupling tensors (KHz) and asymmetry parameters for sulfabenzamide

Model	Nucleus	Method	Basis set	χ_{xx}	χ_{yy}	C_Q	η_Q
Isolated gas-phase[a]	H(1)	B3PW91	6-311+G*	136.51	166.27	−302.78	0.10
			6-311++G**	135.76	163.15	−298.90	0.09
		B3LYP	6-311+G*	129.67	156.71	−300.25	0.11
			6-311++G**	127.45	159.55	−299.95	0.10
	H(2)	B3PW91	6-311+G*	156.51	169.27	−326.78	0.04
			6-311++G**	155.76	169.15	−324.91	0.04
		B3LYP	6-311+G*	159.67	166.71	−326.38	0.03
			6-311++G**	157.45	169.55	−326.95	0.04
	H(3)	B3PW91	6-311+G*	115.45	194.26	−299.71	0.10
			6-311++G**	114.20	195.03	−295.23	0.09
		B3LYP	6-311+G*	116.10	196.69	−284.90	0.09
			6-311++G**	113.08	194.82	−287.90	0.11
	H(4)	B3PW91	6-311+G*	121.13	154.06	−275.19	0.12
			6-311++G**	121.20	155.03	−276.23	0.12
		B3LYP	6-311+G*	119.78	156.19	−275.97	0.13
			6-311++G**	118.28	156.12	−274.40	0.14
Monomer[b]	H(1)	B3PW91	6-311+G*	126.19	163.17	−289.36	0.12
			6-311++G**	125.67	165.23	−290.90	0.14
		B3LYP	6-311+G*	124.47	166.78	−291.25	0.14
			6-311++G**	124.15	163.90	−288.05	0.13
	H(2)	B3PW91	6-311+G*	153.72	166.46	−320.18	0.04
			6-311++G**	154.96	165.06	−320.02	0.04
		B3LYP	6-311+G*	157.93	161.37	−319.30	0.03
			6-311++G**	147.58	169.66	−317.24	0.04
	H(3)	B3PW91	6-311+G*	124.03	186.27	−310.30	0.17
			6-311++G**	125.16	186.15	−311.31	0.18
		B3LYP	6-311+G*	123.27	186.71	−319.98	0.18
			6-311++G**	122.45	189.56	−312.01	0.19
	H(4)	B3PW91	6-311+G*	106.56	138.09	−244.65	0.13
			6-311++G**	104.67	138.59	−243.26	0.14
		B3LYP	6-311+G*	103.37	136.79	−240.16	0.13
			6-311++G**	100.86	135.78	−236.64	0.13
Cluster[c]	H(1)	B3PW91	6-311+G*	78.45	129.41	−207.86	0.24
			6-311++G**	77.21	131.56	−208.77	0.26
		B3LYP	6-311+G*	73.09	130.45	−203.07	0.28
			6-311++G**	71.95	127.73	−199.68	0.28
	H(2)	B3PW91	6-311+G*	157.21	161.21	−318.42	0.02
			6-311++G**	155.70	162.16	−317.86	0.02
		B3LYP	6-311+G*	159.33	162.11	−321.44	0.02
			6-311++G**	157.55	162.35	−319.90	0.02
	H(3)	B3PW91	6-311+G*	96.72	173.73	−270.45	0.29
			6-311++G**	95.56	173.65	−269.35	0.29
		B3LYP	6-311+G*	94.71	174.54	−269.25	0.30
			6-311++G**	94.69	171.70	−266.39	0.30
	H(4)	B3PW91	6-311+G*	74.50	126.34	−200.84	0.26
			6-311++G**	72.56	126.03	−198.59	0.27
		B3LYP	6-311+G*	74.58	124.89	−199.47	0.25
			6-311++G**	73.78	123.81	−197.59	0.25

[a] A fully optimized isolated gas-phase sulfabenzamide at the B3LYP/6-311++G** level of theory.
[b] Crystalline monomer obtained by X-ray coordinates [41] and also optimized hydrogen positions.
[c] The target molecule in cluster.

date. Since LYP is designed to compute the full correlation energy instead of just a correction to local spin density approximation (LSDA), its overall performance is remarkably good [46]. Moreover, various combinations of diffuse and polarization functions being necessary for computation of EFG tensors of hydrogen, nitrogen and oxygen atoms involved in HBs are included in 6-311+G* and 6-311++G** basis sets [47,48]. Hence, for DFT calculations, B3LYP and B3PW91 [49,50] with 6-311+G* and 6-311++G** standard basis sets employed to calculate the EFG tensors. The available crystal coordinates of sulfabenzamide were obtained from X-ray diffraction study [41] and a cluster model consisting of the most possible HB interacting molecules with the target one was created; see Table 1 and Fig. 1 for details. Since the hydrogen atoms do not scatter X-rays effectively, their positions are not known with certainty even for highly resolved crystal structures. As shown both theoretically and experimentally, the NQR parameters and structural properties are mutually correlated [51–54]; thus, the resulted errors in the bond distances and angles of hydrogen atoms due to this uncertainty can have a significant effect on the calculated quadrupole coupling tensors. However, the geometries of just hydrogen atoms were optimized at the level of B3LYP/6-311++G** while those of other atoms remained frozen during the H-optimization process. Furthermore, fully optimization at the level of B3LYP/6-311++G** was performed for an isolated gas-phase of sulfabenzamide, see Table 1. This level of theory has been previously shown to give hydrogen atom position comparable to neutron diffraction values for a variety of systems [55–58]. To have a comparison among the capabilities of various nuclei to contribute in the H-bonding interactions, and also to systematically investigate the H-bonding effects on the ^{14}N, ^{17}O and ^{2}H EFG tensors in sulfabenzamide crystalline structure, all of the EFG calculations were performed for three models of system; an isolated gas-phase, the monomer and the heptameric cluster of sulfabenzamide; see Tables 2–4. Since the EFG tensors, q_{ii}, were calculated in the principal axes system, PAS, ($|q_{zz}|>|q_{yy}|>|q_{xx}|$), Eqs. (1) and (2) were used to evaluate the experimentally measurable NQR parameters, C_Q and η_Q, respectively. The standard values of quadrupole moment, Q, reported by Pyykkö [59] were employed in Eq. (1); $Q(^{17}O)=25.58$ mb, $Q(^{14}N)=20.44$ mb, and $Q(^2H)=2.86$ mb.

$$\chi_{ii}(\mathrm{MHz}) = e^2 Q q_{ii} h^{-1}, \quad i = x, y, z \tag{1}$$

$$C_Q(\mathrm{MHz}) = e^2 Q q_{ZZ} h^{-1}$$
$$\eta_Q = \left|\frac{q_{yy}-q_{xx}}{q_{zz}}\right|, \qquad 0 \le \eta_Q \le 1 \tag{2}$$

Tables 2–4 present the calculated ^{14}N, ^{17}O and ^{2}H C_Q and η_Q parameters for crystalline monomer and the target molecule in crystalline heptameric cluster of sulfabenzamide.

3. Results and discussion

This work studies the various intermolecular HB interactions in the crystal structure of sulfabenzamide by DFT calculations of the EFG tensors at the sites of the ^{14}N, ^{17}O and ^{2}H nuclei in two single and cluster models. As previously Wu and co-workers [60–62] have highlighted the importance of including the whole intermolecular HB network to accurately simulate the components of the EFG tensors, H-bonding effects were considered in the calculations via creating a heptameric cluster of sulfabenzamide using the X-ray coordinates at 293 K. Fig. 1 shows that sulfabenzamide makes various intermolecular hydrogen bonds in the solid phase where the target molecule completely contributes to the H-bonding interactions in cluster model. Therefore, the EFG tensor calculations were performed for three models of optimized isolated gas-phase, crystalline monomer and crystalline heptameric cluster of sulfabenzamide. The calculated EFG tensors were converted to the NQR parameters, C_Q and η_Q, using Eqs. (1) and (2). The summarized results in Tables 2–4 indicate that the calculated values of optimized gas-phase and crystalline monomer are different due to the difference in the structural properties between them, see Table 1. By comparing the results of the monomer and the target molecule in the cluster, the capability of various nuclei in contributing to HBs can easily be compared. In fact, one can easily obtain some trends. First, the χ_{ii} values of those nuclei which participate in the intermolecular H-bonding interactions decrease, but on the other hand, their η_Q values increase from the monomer to the cluster. The magnitude of these changes for each nucleus depends on its contribution to the interactions. Therefore, more changes in each nucleus NQR parameter between the monomer and the target molecule in the cluster indicate its greater role among the other nuclei in contributing to HBs. Second, the calculated parameters with the 6-311++G** and 6-311+G* basis sets are in good consistent with each other. The following text discusses more on the results of this

study where the results of B3LYP/6-311++G** because of the least basis set superposition error, BSSE, [63,64] are referred to.

3.1. Effect of hydrogen bonds on the structural properties

The effect of hydrogen bonds on the structural properties investigated by performing a fully optimization at the level of B3LYP/6-311++G** for an isolated gas-phase of sulfabenzamide and comparing with its crystalline monomer. It should be noted, the monomer was also H-optimized at the B3LYP/6-311G** level, where during this optimization the positions of the hydrogen atoms were allowed to fully relax will those of all other atoms remained frozen. The results are listed in Table 1 show that the geometrical parameters of the optimized isolated gas-phase and crystalline monomer are different. Moreover, different ^{14}N, ^{17}O and ^{2}H EFG tensors were also calculated for two structures which reveal the relationship between NQR parameters and the structural properties which is in agreement with the previous NMR study of Xu and co-workers [65]. Tables 2–4 exhibit more significant difference of EFG tensors for ^{14}N nuclei rather than ^{17}O and ^{2}H nuclei in these two models of sulfabenzamide.

3.2. ^{14}N NQR parameters

In this section, the calculated ^{14}N quadrupole coupling tensors, χ_{ii}, quadrupole coupling constant, C_Q, and asymmetry parameter, η_Q, of the monomer and target molecule in the heptameric crystalline sulfabenzamide are discussed. As shown in Fig. 1b, the N(1) and N(2) sites contribute in the N–H(1–1)…O=C(3–2) and N–H(2–3)…O=C(3–6) hydrogen bonds, respectively. Due to this contribution to HB interaction, ^{14}N quadrupole coupling tensors for the target molecule in the cluster deviate significantly from the monomer values. As can be seen in Table 2, both χ_{xx} and χ_{yy} tensor components increase from the monomer to the cluster whereas χ_{zz} or C_Q exhibits opposite tendency. This is also reflected in the calculated asymmetry parameter. As a general trend, from the monomer to the target molecule in the cluster, H-bonding interactions reduce the calculated ^{14}N quadrupole coupling constant values whereas increase the asymmetry parameter.

As shown in Table 2, H-bonding interactions have a different influence on the ^{14}N quadrupole coupling tensor. N(1) site contributes to N(1)–H(1)…O(3–2) HB interaction and with 1.02 MHz reduction in the C_Q value, ΔC_Q(N1)=1.02 MHz, is the most affected nucleus from the monomer to the target molecule in the heptameric cluster. On the other hand, the change in other principal components of the ^{14}N (1) quadrupole coupling tensor, χ_{xx} and χ_{yy}, and asymmetry parameter is also remarkable; see Table 2. The values of asymmetry parameter at N(1) site show also a significant dependency on the hydrogen bonding interactions. When the N(1)–H(1)…O=C(3–2) interaction is considered in the heptameric model, the η_Q values of N(1) nucleus increase 0.26 from the monomer to the target molecule. These effects suggest that the intermolecular hydrogen bond interaction at the N(1) site in crystalline sulfabenzamide is rather strong; $r_{N1\cdots O3-2}$=2.69 Å.

For the quadrupole coupling tensors at the N(2) site, the comparison of the monomer and the heptameric cluster shows some discrepancy, although not as dramatic as the one seen for N(1). By a quick look at the Fig. 1b, it is found that N(2) atom of the target molecule can form an intermolecular hydrogen bond with molecule number 6, which is located at an adjacent anti-parallel chain. From having only one possibility to formation of hydrogen bond, $r_{N(2)\cdots O(3-6)}$=2.85 Å, C_Q and η_Q values for N(2) change by 0.75 MHz and 0.25 units from the monomer to the target molecule in the cluster, ΔC_Q(N2)=0.75 MHz and $\Delta\eta_Q$(N2)=0.25, respectively. While EFG tensor at N(2) site is approximately axially symmetric, $\eta_Q \approx 0$, for the gas-phase isolated molecule, and also remains almost symmetrical from the optimized gas-phase molecule to the monomer molecule in solid phase, this tensor becomes almost asymmetric for the target molecule in the heptameric cluster, $\eta_Q \approx 0.4$. As can be seen from Table 2, including the neighboring molecules, η_Q values of N(1) and N(2) change by 0.26 and 0.25 units from the monomer to the target molecule in the cluster, respectively. We calculated similar results previously for the ^{14}N NQR parameters of sulfamerazine [39]. It is noted that to the best of our knowledge, no experimental ^{14}N NQR data were available for sulfabenzamide in the literature. However, the obtained results clearly indicate that, despite N(2), N(1) contributes more effectively to HB interactions in the cluster model of sulfabenzamide. Thus, N(1)–H(1)…O(3–2) HB interactions play an important role in crystalline sulfabenzamide such as its polymorphism, tableting behavior, and drug activity.

3.3. ^{17}O NQR parameters

As a general trend seen from previous section, the amount of changes in the ^{14}N quadrupole coupling tensor eigenvalues depends; directly on the participation of the nucleus in the intermolecular H-bonding interactions. In this section, we focus on the results obtained for ^{17}O quadrupole coupling tensor; see Table 3.

Being in agreement with the previous calculations, the changes in the ^{17}O quadrupole coupling tensor are also significant. As seen form Table 3, both χ_{yy} and χ_{zz} tensor components decrease from the monomer to the cluster whereas χ_{xx} exhibits opposite tendency. As a general trend, from the monomer to the target molecule in the cluster, HB interactions reduce the calculated ^{17}O quadrupole coupling constant values, C_Q(^{17}O), whereas they increase the asymmetry parameter. Fig. 1 illustrates that the thionyl groups of the target molecule in cluster of sulfabenzamide interact with two neighboring molecules. O(1) and O(2) sites of the target in heptameric cluster contribute to O(1)…N(1–7), $r_{O\cdots N}$=2.81 Å, and O(2)…C(2–3), $r_{O\cdots C}$=2.98 Å, hydrogen bonds, respectively. Due to the contribution to HB interactions, C_Q and η_Q values of O(1) change by 0.46 MHz reduction and 0.13 units increase from monomer to the cluster, respectively. On the other hand, C_Q value of O(2) reduces 0.2 MHz whereas η_Q value increases 0.08 from monomer to the target molecule in heptameric cluster, which are less significant than the changes of O(1). This trend reveals the greater role of O(1) in contribution to HB while that of O(2) is smaller.

By a quick look at the Fig. 1b, it is found that O(3) atom of the target molecule can form an intermolecular hydrogen bond with molecule number 4. From having only one possibility to formation of hydrogen bond, $r_{O(3)\cdots N(1-4)}$=2.74 Å, C_Q and η_Q values for O(3) change by 0.74 MHz and 0.38 units from the monomer to the target molecule in the cluster, respectively. Table 3 shows that component C_Q of O(3) with approximately 2.42 MHz reduction is the most affected component where changes in the other components are small. It is also remarkable that O(3) with ΔC_Q=0.74 MHz and $\Delta\eta_Q$=0.38 units is the most affected nucleus from the monomer to the target molecule in the heptameric cluster. This trend reveals the major role of O(3) in contribution to HBs in the cluster. It is noted that to our knowledge no experimental ^{17}O NQR data are available for sulfabenzamide in the literature.

3.4. ^{2}H NQR parameters

As discussed in the previous sections, including the H-bonding interactions has a remarkable effect on the calculated ^{14}N and ^{17}O nuclear quadrupole coupling tensors. Table 4 shows the calculated ^{2}H quadrupole coupling values at the hydrogen sites for sulfabenzamide in the isolated gas phase, monomer and the target molecule in the heptameric cluster. From Table 4, one can see the effect of HBs on ^{2}H nuclear quadrupole coupling constants. Comparison of the magnitudes of NQR parameters of Tables 2–4 reveals that these magnitudes for ^{2}H are less than those of ^{14}N and ^{17}O nuclei because the hydrogen nucleus feels a lower electron density comparing to those of ^{14}N and ^{17}O. However, since the EFG tensors are very sensitive to the electronic

site of quadrupole nucleus, the influence of the HB interactions on the EFG tensors at the sites of ^{2}H nuclei are observed in Table 4. The target sulfabenzamide molecule makes three HBs with the acceptor molecules at (x, y, 1/2+z), (−x, 1/2−y, −z) and (−x, y, 1/2+z); therefore, due to the participation in the H-bonding interactions, the change in the ^{2}H quadrupole values is rather significant.

As Fig. 1b indicates, the hydrogen bond at the –NH_2 site of the target molecule involves O(3–2) atom of neighboring molecule. Thus, For H(1) nucleus, the C_Q and η_Q values change approximately 88.37 kHz and 0.15 units, respectively, depending on whether it is in the isolated monomer or in the H-bonding environment. These features reveal the major role of –NH_2 group in contribution to the intermolecular H-bonding interactions of the crystalline sulfabenzamide. In fact, H(1) with a remarkable ΔC_Q of 88.37 kHz and $\Delta\eta_Q$ of 0.15 units is the most affected nucleus of sulfabenzamide in the H-bonding interactions. H(3), $r_{H3\ldots O(3-6)}$ = 1.85 Å, is the next affected nucleus of target molecule in the hydrogen bonding interactions. As one can see from Table 4, for H(3) site, C_Q reduces 45.62 kHz and η_Q increases 0.11 units from monomer to the target in cluster.

For the H(4) site, the H-bonding interactions make 39 kHz reduction and 0.12 units increase in C_Q and η_Q values, respectively. On the other hand, in contrast to the changes of EFG tensors at the sites of H(1), H(3) and H(4) nuclei due to the HB interactions, these tensors at the H(2) site of the target molecule are almost remained unchanged because this nucleus dos not contribute to any HB interactions in the cluster. However, including the neighboring molecules, C_Q and η_Q values of H(2) change only by 2.7 kHz and 0.02 from the monomer to the target molecule in the cluster, respectively. As mentioned in the previous sections, N(1) and O(3) have the major contribution to HB interactions in the cluster which, as a result, the NQR parameters at the sites of H(1) and H(3) are also significantly influenced.

4. Conclusion

We have presented a systematic computational study on the HB interactions of sulfabenzamide crystal structure by DFT calculations of EFG tensors at the sites of ^{14}N, ^{17}O and ^{2}H nuclei in two monomer and cluster models. The results reveal that the EFG tensors at the sites of nitrogen, oxygen and hydrogen nuclei are influenced by HB interactions and are such appropriate parameters to characterize the properties of these interactions. The target molecule contributes to N–H…O and C–H…O types of HB interactions in the cluster model while the EFG tensors at the sites of various nuclei are not similarly influenced by these interactions. Among the other nuclei of sulfabenzamide, N(1), O(3) and H(1) are those nuclei which their EFG tensors are significantly influenced by HB interactions. In other words, N–H…O type HBs are more effective than C–H…O type in controlling the crystal packing, tableting behavior and drug activity of sulfonamides. As a final note, the results of B3LYP and B3PW91 show good agreement in the parameter discrepancies from the isolated gas-phase to the cluster.

References

[1] S. Scheiner, T. Kar, J. Pattanayak, Comparison of various types of hydrogen bonds involving aromatic amino acids, J. Am. Chem. Soc. 124 (2002) 13257–13264.
[2] A.V. Finkelstein, O.B. Ptitsyn, Protein Physics, Academic Press, London, 2002.
[3] G.A. Jeffery, W. Saenger, Hydrogen Bonding in Biological Structures, Springer-Verlag, Berlin, 1991.
[4] D.A. Adsmond, D.J.W. Grant, Hydrogen bonding in sulfonamides, J. Pharm. Sci. 90 (2001) 2058–2077.
[5] S.S. Yang, J.K. Guillory, Polymorphism in sulfonamides, J. Pharm. Sci. 61 (1972) 26–40.
[6] C. Sun, D.J.W. Grant, Influence of crystal structure on the tableting properties of sulfamerazine polymorphs, Pharm. Res. 18 (2001) 274–280.
[7] R.S. Lipsitz, Y. Sharma, B.R. Brooks, N. Tjandra, Hydrogen bonding in high-resolution protein structures: a new method to assess NMR protein geometry, J. Am. Chem. Soc. 124 (2002) 10621–10626.
[8] M. Strohmeier, D. Stueber, D.M. Grant, Accurate ^{13}C and ^{15}N chemical shift and ^{14}N quadrupolar coupling constant calculations in amino acid crystals: zwitterionic, hydrogen-bonded systems, J. Phys. Chem., A 107 (2003) 7629–7635.
[9] M.J. Hunt, A.L. Mackay, Deuterium and nitrogen pure quadrupole resonance in deuterated amino acids, J. Magn. Reson. 15 (1974) 402–406.
[10] B. Nogaj, Hydrogen-bond theories and models based on nuclear quadrupole resonance spectroscopy studies, J. Phys. Chem. 91 (1987) 5863–5869.
[11] S.E. Ashbrook, M.J. Duer, Structural information from quadrupolar nuclei in solid state NMR, Concepts Magn. Reson., A 28 (2006) 183–248.
[12] R. Bersohn, Nuclear electric quadrupole spectra in solids, J. Chem. Phys. 20 (1952) 1505–1509.
[13] M.H. Cohen, F. Reif, Quadrupole effects in nuclear magnetic resonance studies of solids, Solid State Phys. 5 (1957) 321–438.
[14] M.J. Duer, Introduction to Solid-state NMR Spectroscopy, Blackwell Science, Oxford, 2004.
[15] C.P. Slichter, Principles of Magnetic Resonance, Harper and Row, London, 1992.
[16] T.H. Maren, Relations between structure and biological activity of sulfonamides, Annu. Rev. Pharmacol. Toxicol. 16 (1976) 309–327.
[17] R.J. Mesley, E.E. Houghton, Infrared identification of pharmaceutically important sulfonamides with particular reference to the occurrence of polymorphism, J. Pharm. Pharmacol. 19 (1967) 295–304.
[18] Y. Funahashi, N.H. Sugi, T. Semba, Y. Yamamonoto, S. Hamaoka, N.T. Tamai, Y. Ozawa, A. Tsuruoka, K. Nara, K. Takahashi, T. Kabe, J. Kamata, T. Owa, N. Veda, T. Haneda, M. Yonega, K. Yoshimatsu, T. Wakabayashi, Sulfonamide derivative, E7820, is a unique angiogenesis inhibitor suppressing an expression of integrin alpha2 subunit on endothelium, Cancer Res. 62 (2002) 6116–6123.
[19] T. Semba, Y. Funahashi, N. Ona, Y. Yamamoto, N.H. Sugi, M. Asada, K. Yoshimatsu, T. Wakabayashi, An angiogenesis inhibitor E7820 shows broad-spectrum tumor growth inhibition in a xenograft model: possible value of integrin alpha2 on platelets as a biological marker, Clin. Res. 10 (2004) 1430–1438.
[20] J. Slawinski, M. Gdaniec, Synthesis, molecular structure, and in vitro antitumor activity of new 4-chloro-2-mercaptobenzenesulfonamide derivatives, Eur. J. Med. Chem. 40 (2005) 377–389.
[21] Q. Chen, P.N.P. Rao, E.E. Knaus, Design, synthesis, and biological evaluation of N-acetyl-2-carboxybenzenesulfonamides: a novel class of cyclooxygenase-2 (COX-2) inhibitors, Bioorg. Med. Chem. 13 (2005) 2459–2468.
[22] A.K. Gadad, M.N. Noolyi, R.V. Karpoormath, Synthesis and anti-tubercular activity of a series of 2-sulfonamido/trifluoromethyl-6-substituted imidazo[2,1-b]-1,3,4-thiadiazole derivatives, Bioorg. Med. Chem. 12 (2004) 5651–5659.
[23] V.K. Agrawel, S. Bano, C.T. Supuran, P.V. Khadikar, QSAR study on carbonic anhydrase inhibitors: aromatic/heterocyclic sulfonamides containing 8-quinoline-sulfonyl moieties, with topical activity as antiglaucoma agents, Eur. J. Med. Chem. 39 (2004) 593–600.
[24] C.M. Yeung, L.L. Klein, C.A. Flentge, J.T. Randolph, C. Zhao, M. Sun, T. Dekhtyar, V.S. Stoll, D.J. Kempf, Oximinoarylsulfonamides as potent HIV protease inhibitors, Bioorg. Med. Chem. Lett. 15 (2005) 2275–2278.
[25] I. Encio, D.J. Morre, R. Villar, M.J. Gill, V.M. Merino, Benzo[b] thiophenesulphonamide 1,1-dioxide derivatives inhibit tNOX activity in a redox state-dependent manner, Br. J. Cancer 92 (2005) 690–695.
[26] M.J. Nieta, F.L. Alovero, R.H. Manzo, M.R. Mazzieri, Benzenesulfonamide analogs of fluoroquinolones: antibacterial activity and QSAR studies, Eur. J. Med. Chem. 40 (2005) 361–369.
[27] J.N. Dominguez, C. Leon, J. Rodrigues, N.G. Dominguez, J. Gut, D.J. Rosethal, Synthesis and anti-malarial activity of sulfonamide chalcone derivatives, Farmaco 60 (2005) 307–311.
[28] G.M. Golzar, A new polymorph of sulfamerazine, Acta Crystallogr., Sect. E 62 (2006) 2166–2167.
[29] C. Emperini, A. Ecchi, A. Scozzafava, C.T. Supuran, Carbonic anhydrase inhibitors. Interaction of indapamide and related diuretics with 12 mammalian isozymes and X-ray crystallographic studies for the indapamide-isozyme II adduct, Bioorg. Med. Chem. Lett. 18 (2008) 2567–2573.
[30] A. Innocenti, A. Maresca, A. Scozzafava, C.T. Supuran, Carbonic anhydrase inhibitors: thioxolone versus sulfonamides for obtaining isozyme-selective inhibitors? Bioorg. Med. Chem. Lett. 18 (2008) 3938–3941.
[31] J. Turczan, T. Medwick, Identification of sulfonamides by NMR spectroscopy, J. Pharm. Sci. 61 (1972) 434–443.
[32] D.S. Hughes, M.B.T. Hursthouse, T. Trelfall, S. Tavener, A new polymorph of sulfathiazole, Acta Crystallogr., Sect C 55 (1999) 1831–1833.
[33] A. Portieri, R.K. Harris, R.A. Fletton, R.W. Lancaster, T.L. Threlfall, Effects of polymorphic differences for sulfanilamide, as seen through 13C and 15N solid-state NMR, together with shielding calculations, Magn. Reson. Chem. 42 (2004) 313–320.
[34] K.R. Acharya, K.N. Kuchela, G. Kartha, Crystal structure of sulfamerazine, J. Crystallogr. Spectrosc. Res. 12 (1982) 369–376.
[35] X. Cao, C. Sun, T.J. Thamann, A study of sulfamerazine single crystals using atomic force microscopy, transmission light microscopy, and Raman spectroscopy, J. Pharm. Sci. 94 (2005) 1881–1892.
[36] S.C. Péreza, L. Cerionia, A.E. Wolfensona, S. Faudoneb, S.L. Cuffini, Utilization of pure nuclear quadrupole resonance spectroscopy for the study of pharmaceutical crystal forms, Int. J. Pharmacol. 298 (2005) 143–152.
[37] J. Seliger, V. Zagar, R. Blinc, A new highly sensitive ^{1}H–^{14}N nuclear-quadrupole double-resonance technique, J. Magn. Reson. 106 (1994) 214–222.
[38] H.N. Kosutić, A. Danilovski, D. Filić, M. Marinković, E. Mestrović, M. Dumić, Supramolecular structures of three isomeric 4-(methylphenylamino)pyridine-3-sulfonamides, Acta Crystallogr., Sect. C 11 (2005) 648–651.
[39] M. Aghazadeh, M. Mirzaei, Hydrogen bond interactions in sulfamerazine: DFT study of the O-17, N-14 and H-2 electric field gradient tensors, Chem. Phys. 351 (2008) 159–162.

[40] R. Blinc, J. Seliger, A. zidansek, V. Zagar, F. Milia, H. Robert, ^{14}N nuclear quadrupole resonance of some sulfa drugs, Solid State Nucl Magn. Reson. 30 (2006) 61–68.
[41] J. Rambaud, R. Roques, S. Alberola, F. Sabon, Structure cristalline et moleculaire du sulfabenzamide, Bull. Soc. Chim. Fr. (1980) 51–55.
[42] M.J. Frisch, G.W. Trucks, H.B. Schlegel, G.E. Scuseria, M.A. Robb, J.R. Cheeseman, V.G. Zakrzewski, J.A. Montgomery, R.E. Stratmann, J.C. Burant, S. Dapprich, J.M. Millam, A.D. Daniels, K.N. Kudin, M.C. Strain, O. Farkas, J. Tomasi, V. Barone, M. Cossi, R. Cammi, B. Mennucci, C. Pomelli, C. Adamo, S. Clifford, J. Ochterski, G.A. Petersson, P.Y. Ayala, Q. Cui, K. Morokuma, D.K. Malick, A.D. Rabuck, K. Raghavachari, J.B. Foresman, J. Cioslowski, J.V. Ortiz, A.G. Baboul, B.B. Stefanov, G. Liu, A. Liashenko, P. Piskorz, I. Komaromi, R. Gomperts, R.L. Martin, D.J. Fox, T. Keith, M.A. Al-Laham, C.Y. Peng, A. Nanayakkara, C. Gonzalez, M. Challacombe, P.M.W. Gill, B. Johnson, W. Chen, M.W. Wong, J.L. Andres, C. Gonzalez, M. Head-Gordon, E.S. Replogle, J.A. Pople, Gaussian 98, Gaussian Inc., Pittsburgh, PA, 1998.
[43] M. Köster, P. Calaminici, N. Russo, Nuclear quadrupole coupling constants from the Gaussian density-functional method, Phys. Rev., A 53 (1996) 3865–3868.
[44] G. De Luca, N. Russo, A.M. Köster, P. Calaminici, K. Jug, Density functional theory calculations of nuclear quadrupole coupling constants with calibrated 17O quadrupole moments, Mol. Phys. 97 (1999) 347–354.
[45] E. Sicilia, G. De Luca, S. Chiodo, N. Russo, P. Calaminici, A.M. Köster, K. Jug, Density functional calculations of nuclear quadrupole coupling constants with calibrated ^{14}N quadrupole moments, Mol. Phys. 99 (2001) 1039–1051.
[46] C.J. Cramer, Essentials of Computational Chemistry, Wiley, Pittsburg, PA, 1998.
[47] R.G. Parr, W. Yang, Density-functional Theory of Atoms and Molecules, Oxford Univ. Press, Oxford, 1989.
[48] A.D. McLean, G.S. Chandler, Contracted Gaussian basis sets for molecular calculations. I. Second row atoms, Z=11–18, J. Chem. Phys. 72 (1980) 5639–5644.
[49] A.D. Becke, Density-functional thermochemistry. III. The role of exact exchange, J. Chem. Phys. 98 (1993) 5648–5652.
[50] C. Lee, W. Yang, R.G. Parr, Development of the Colle–Salvetti correlation-energy formula into a functional of the electron density, Phys. Rev., B 37 (1988) 785–789.
[51] J.P. Perdew, Y. Wang, Accurate and simple analytic representation of the electron-gas correlation energy, Phys. Rev., B 45 (1992) 13244–13249.
[52] T.M. Clark, P.J. Grandinetti, Dependence of bridging oxygen O-17 quadrupolar coupling parameters on Si–O distance and Si–O–Si angle, J. Phys., Condens. Matter (2003) 2387–2395.
[53] K.E. Vermillion, P. Florian, P.J. Grandinetti, Relationships between bridging oxygen O-17 quadrupolar coupling parameters and structure in alkali silicates, J. Chem. Phys. 108 (1998) 7274–7285.
[54] A. Pepels, H. Gunther, J.P. Amoureux, Li-7 solid-state NMR of organolithium compounds: dependence of Li-7 quadrupolar coupling, chi(Li-7), on the structural angle C–Li–C, J. Am. Chem. Soc. 122 (2000) 9858–9859.
[55] S. Ono, T. Taguma, S. Kuroki, I. Ando, A study of hydrogen-bonding of amino acids, peptides and polypeptides in the solid state as a function of temperature by static ^{2}H NMR method, J. Mol. Struct. 602 (2002) 49–58.
[56] J.K. Harper, G. McGeorge, D.M. Grant, Solid-state 13C chemical shift tensors in terpenes. 2. NMR characterization of distinct molecules in the asymmetric unit and steric influences on shift in parthenoide, J. Am. Chem. Soc. 121 (1999) 6488–6496.
[57] A.D. Becke, Density-functional thermochemistry. III. The role of exact exchange, J. Chem. Phys. 98 (1993) 5648–5652.
[58] J.C. Facelli, Density functional theory calculations of the structure and the bacteriochlorophyll a, J. Phys. Chem., B 102 (1998) 2111–2116.
[59] P. Pyykkö, Spectroscopic nuclear quadrupole moment, Mol. Phys. 99 (2001) 1617–1629.
[60] S. Dong, R. Ida, G. Wu, A combined experimental and theoretical ^{17}O NMR study of crystalline urea: an example of large hydrogen bond effects, J. Phys. Chem., A 104 (2000) 11194–11202.
[61] G. Wu, K. Yamada, A. Dong, H. Grondey, Intermolecular hydrogen bonding effects on the amide oxygen electric-field-gradient and chemical shielding tensors of benzamide, J. Am. Chem. Soc. 122 (2000) 4215–4216.
[62] G. Wu, S. Dong, R. Ida, N. Reen, A solid-state ^{17}O nuclear magnetic resonance study of nucleic acid bases, J. Am. Chem. Soc. 124 (2002) 1768–1777.
[63] M. Mirzaei, F. Elmi, N.L. Hadipour, A systematic investigation of hydrogen-bonding effects on the ^{17}O, ^{14}N, and ^{2}H nuclear quadrupole resonance parameters of anhydrous and monohydrated cytosine crystalline structures: a density functional theory study, J. Chem. Phys., B 110 (2006) 10991–10996.
[64] M. Mirzaei, N.L. Hadipour, A computational NQR study on the hydrogen-bonded lattice of cytosine-5-acetic acid, J. Comput. Chem. 29 (2008) 832–838.
[65] X.-P. Xu, S.C.F. Au-Yeung, Investigation of chemical shift and structure relationships in nucleic acids using NMR and density functional theory methods, J. Phys. Chem., B 104 (2000) 5641–5650.